

## Coexistence of low-frequency fluctuations and stable emission on a single high-gain mode in semiconductor lasers with external optical feedback

T. Heil, I. Fischer, and W. Elsäßer

*Institut für Angewandte Physik, Technische Universität Darmstadt, Schlossgartenstrasse 7, D-64289 Darmstadt, Germany*

(Received 5 December 1997)

We present a systematic investigation of the dynamical behavior of semiconductor lasers subject to external optical feedback dependent on the injection current and the optical feedback strength. We identify the regimes of low-frequency fluctuations (LFFs), fully developed coherence collapse, and a large regime of the coexistence of LFFs and stable emission on single high-gain external-cavity mode extending over more than one order of magnitude of optical feedback strengths. Thus, we provide experimental evidence for one major prediction of the theoretical model based on the Lang-Kobayashi equations, which proposes a deterministic mechanism underlying the LFFs. [S1050-2947(98)50610-5]

PACS number(s): 42.65.Sf, 42.55.Px

Semiconductor lasers, subject to optical feedback from an external cavity, show a variety of dynamical effects in combination with a drastic increase in optical linewidth. Therefore, these dynamical effects are referred to as coherence collapse [1]. The most striking phenomenon within the coherence collapse regime is the onset of irregular fluctuations of the laser intensity on micro- to nanosecond time scales. These time scales are long compared to the other dynamical time scales involved in semiconductor laser dynamics, such as the frequency of the relaxation oscillations or the external cavity round-trip time. Consequently, these irregular fluctuations have been called low-frequency fluctuations (LFF). According to the coarse classification of the regimes of laser operation provided by [2], the coherence collapse, including the LFF phenomenon, corresponds to the chaotic emission regime IV, in which the LFF occur close to the transition to the stable emission regime V, as previous experiments have shown [3].

During the last few years, the mechanism underlying the LFF has prompted lively discussion. In [4], a noise-driven multimode traveling-wave model has been proposed. Also considering the influence of noise, the LFF have been treated in terms of a first-passage time problem [5,6]. Furthermore, the responsible mechanism has been attributed to cavity misalignment [7], and to dynamic changes of the coherence properties of the emitted light [8]. Finally, the LFF have been interpreted as type-II intermittency [9]. Very recently, some of the problems concerning the models mentioned above have been discussed by considering the statistics of the LFF power-dropout events [10]. In 1994, the LFF have been explained as a chaotic itinerancy with a drift [11]. This deterministic model of the LFF is based upon an analysis of the Lang-Kobayashi equations [12], i.e., two coupled delay-differential equations, describing a single-mode semiconductor laser subject to moderate optical feedback from an external cavity.

In this paper, we present a systematic investigation of the dynamical behavior of the system dependent on the two for the dynamics' most relevant parameters: the injection current  $I$  and the optical feedback strength  $\gamma$ . By varying these two parameters over the whole accessible range, we obtain a detailed diagram mapping the dynamical behavior of the sys-

tem in the  $\gamma$ - $I$  space. In particular, we identify four different dynamical regimes: the stable emission regime V, the LFF regime, the fully developed coherence collapse regime, and, to our knowledge for the first time, a large regime of coexistence of LFF and a state of stable emission on a single high-gain external-cavity mode, which extends over more than one order of magnitude of optical feedback strength. In fact, this coexistence of LFF and stable emission on a single high-gain external-cavity mode, occurring over wide parameter ranges, corresponds to a major prediction of the deterministic model of the LFF [13]. Finally, we discuss the influence of the number of longitudinal diode modes on the dynamics of the system, and the impact of spontaneous emission noise on the stability of the stable emission state.

An analysis of the Lang-Kobayashi equations shows that the eigenmodes of the system, consisting of the semiconductor laser cavity and the external cavity, always occur in pairs of stable and unstable fixed points. The stable solutions correspond to constructive interference conditions of the coupled cavities and are usually referred to as modes of the external cavity; the unstable solutions correspond to destructive interference conditions of the coupled cavities and, thus, are called antimodes. The strong nonlinearities of the semiconductor material, as expressed by the linewidth-enhancement factor [14], make modes and antimodes lie on an ellipse around the solitary laser mode in the frequency-inversion space [15]; a linear stability analysis shows that the modes destabilize for increasing optical feedback via Hopf bifurcations, except for at least one mode on the low-frequency, high-gain side of the ellipse, which always remains stable [13]. According to the deterministic model, the chaotic itinerancy takes place along the attractor ruins of the destabilized modes with a drift towards one of these stable high-gain modes (HGMs), so that the emitted power that is organized in irregular picosecond pulses [15] builds up during the itinerancy. As the trajectory iterates towards the high gain part of the ellipse, the basin boundaries of the attractor ruins of modes and antimodes approach, so that even a collision of these attractor ruins can occur, a process that is referred to as crisis. The characteristic dropouts of the emitted power are then associated with such a crisis bounc-

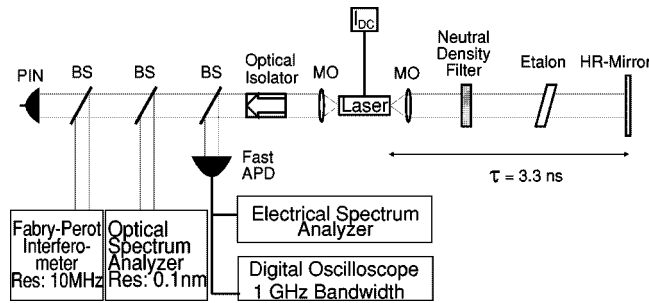


FIG. 1. Experimental setup. The feedback branch on the right-hand side consists of a high reflecting mirror forming the external cavity, an etalon, and a neutral density filter to vary the amount of optical feedback. In the detection branch on the left-hand side, time series, power spectrum, and optical spectrum on different spectral and temporal resolution scales are detected.

ing the trajectory away from its moving drift, towards one of the HGMs, and reinjecting the trajectory into the lower gain part of the ellipse. This deterministic mechanism of the LFFs has been confirmed by streak camera measurements of the picosecond pulsing behavior of the emitted power in the LFF regime [16]. Up to now, the trajectory has always been observed to undergo a crisis, corresponding to a dropout in laser power before the chaotic itinerancy of the trajectory could come to an end by reaching one of the HGMs. Therefore, the name “Sisyphus effect” has been chosen as a synonym for this dynamical behavior. However, our measurements show that the trajectory can, in fact, reach one of these HGMs.

The experiments have been carried out using a Hitachi HLP 1400 laser diode, which is best known with respect to nonlinear studies of external optical feedback. Figure 1 shows the experimental setup. The laser diode is driven by an ultra-low-noise dc-current source and the temperature is stabilized to better than 0.01 K. The beam is collimated by an antireflection-coated microscope objective. The feedback branch consists of a high reflection mirror of interferometric flatness better than  $\lambda/200$ , a neutral density filter to vary the optical feedback strength, and an intracavity etalon with a transmission linewidth of approximately 5 nm, restricting the dynamics of the system to essentially one longitudinal diode mode. The delay time  $\tau$  of the external cavity amounts to  $\tau = 3.3$  ns, which corresponds to an external-cavity mode spacing of 300 MHz. The time-averaged laser intensity is measured by a *p-i-n* photodiode. Both the time series of the intensity and the optical spectrum of the laser are simultaneously measured on two different resolution stages in order to account for the wide temporal and optical scales of the investigated dynamics. The intensity dynamics is detected by a fast avalanche photodiode (APD) with larger than 3-GHz bandwidth. The power spectrum of the APD signal is recorded by an electrical spectrum analyzer of 0.1 kHz to 21 GHz bandwidth. The corresponding time series are low-pass filtered with the cutoff frequency at 1 GHz and detected by a fast digital oscilloscope of the same bandwidth. The optical spectrum is detected by a grating spectrometer with a resolution of 0.1 nm in order to resolve the longitudinal diode modes, and a confocal scanning Fabry-Pérot interferometer to resolve the external cavity modes. The free spectral range of the interferometer amounts to 2 GHz; its resolution to 10

MHz. The optical isolator shields the laser from unwanted external feedback from the detection branch.

In order to map the dynamics of the system in phase space, we have performed the experiment in the following way. The feedback strength  $\gamma$  is adjusted by using a variable neutral density filter. According to the definition of  $\gamma$  given in [12], we calibrate the feedback strength by measuring the effective power reflectivity of the feedback branch. Subsequently, the injection current  $I$  is increased, starting below threshold, over the whole accessible range. The resulting dynamical behavior is investigated and classified depending on the injection current. Repeating this procedure for several different values of feedback strength ranging over three orders of magnitude, we obtain a map of the dynamical behavior of a semiconductor laser subject to optical feedback in the  $\gamma$ - $I$  space, which is depicted in Fig. 2.

The etalon forces the laser to emit on one longitudinal diode mode at the gain maximum,  $\lambda = 840$  nm in this case. Increasing the injection current along the vertical dotted line from A to B depicted in Fig. 2, corresponding to a feedback rate of  $\gamma \approx 25$  ns<sup>-1</sup>, one reaches every dynamical regime present in the  $\gamma$ - $I$  space: After passing the feedback reduced laser threshold, the system enters the stable emission regime V, which, as shown by [17], can be reached in a narrow current interval close to threshold even for uncoated laser diodes. The laser emission is stable on a single longitudinal diode mode and several external-cavity modes. The mode beatings of the external-cavity modes appear as sharp peaks in the power spectrum. The LFF regime is reached by increasing the injection current by approximately 1 mA above threshold. There, a dominant low-frequency contribution builds up in the power spectrum; the external-cavity mode beatings broaden significantly. Restricted by the transmission of the etalon, the emission of the laser is still dominated by one longitudinal diode mode. Figure 3(a) shows a time series of the dynamical behavior within the LFF regime. With increasing injection current, the time intervals between the dropouts decrease. Finally, a continuous transition to the fully developed coherence collapse takes place, accompanied by a broad power spectrum and completely irregular intensity time series. This dynamical behavior is demonstrated by Figs. 3(b) and 3(c), showing a time series of the transition regime and the fully developed coherence collapse regime, respectively. However, the most striking aspect of this  $\gamma$ - $I$  space diagram is the existence of a large region within the LFF regime, where discrete transitions between LFF and stable emission on a single external-cavity mode occur.

In the following, we will focus on this coexistence region embedded in the LFF regime. In a snapshotlike picture, Fig. 4 shows the intensity time series of a transition from the LFF state to the stable emission state occurring at the time of 3  $\mu$ s. The important features accompanied by this transition are, first, that the intensity of the laser stabilizes on a higher level than the LFF. Accordingly, the transition to stable emission is characterized by a sudden increase in the time-averaged intensity recorded by the *p-i-n* photodiode. Second, the power spectrum is completely flat; no frequency components remain. Third, the stable emission occurs on a single external-cavity mode, resolved by the scanning Fabry-Pérot interferometer. The inset of Fig. 4 depicts the optical spectrum of the stable emission state showing a single sharp peak

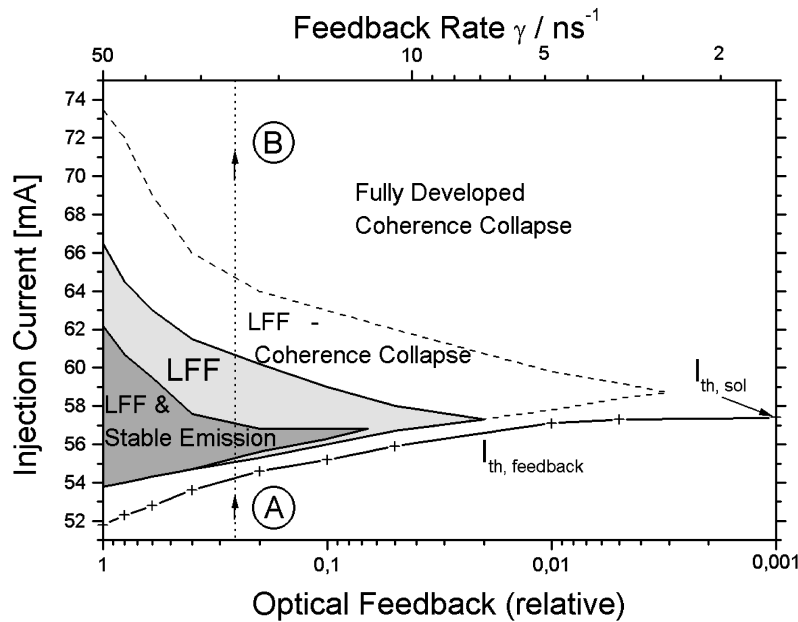


FIG. 2. The dynamical behavior of a semiconductor laser subject to optical feedback in feedback ( $\gamma$ )-current ( $I$ ) space. The LFF regime is depicted in light gray. The dark-gray region embedded in the LFF regime corresponds to the region of coexistence of the stable emission state and the LFF state. The unshaded region encompassed by the dashed line corresponds to the continuous transition between the LFF regime and the fully developed coherence collapse regime.

whose width is limited only by the resolution of the Fabry-Pérot interferometer. The time interval required to perform such a frequency scan amounts to 5 ms, during which, as shown by the inset, the laser emits on a single external-cavity mode. Keeping the very fast dynamics of semiconductor lasers in mind, this time interval is extremely long. For certain parameter ranges, we observe durations of stable states ex-

ceeding 1 min, which is more than  $10^8$  times longer than the typical time intervals between two subsequent LFF events under identical conditions. Thus, a semiconductor laser subject to optical feedback can remain stable on a single high-gain external-cavity mode within the LFF regime for very long times. This measurement is the experimental evidence for the existence of the HGMs over wide parameter ranges within regime IV, which has been predicted by [13]. The trajectory of the system reaches the stable mode after its chaotic itinerancy. And so, despite greek mythology, “Sisyphus can reach his goal and remain there.”

The time intervals of stable emission are prolonged for stronger feedback and higher injection currents. Only a few tenths of mA above laser threshold, the duration of the stable states is comparable to the time interval between two subse-

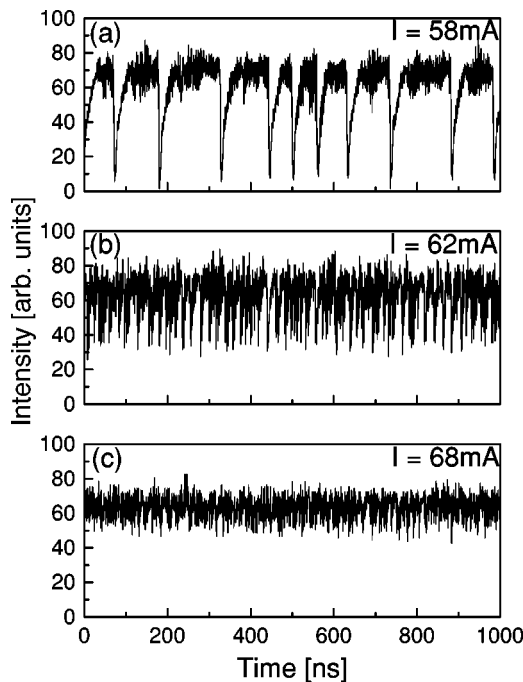


FIG. 3. Intensity time series of a semiconductor laser subject to constant optical feedback and three different injection currents. The optical feedback amounts to  $\gamma \approx 25 \text{ ns}^{-1}$ , which corresponds to the vertical line from A to B depicted in Fig. 2. The injection currents applied to the laser are (a) 58 mA, (b) 62 mA, and (c) 68 mA.

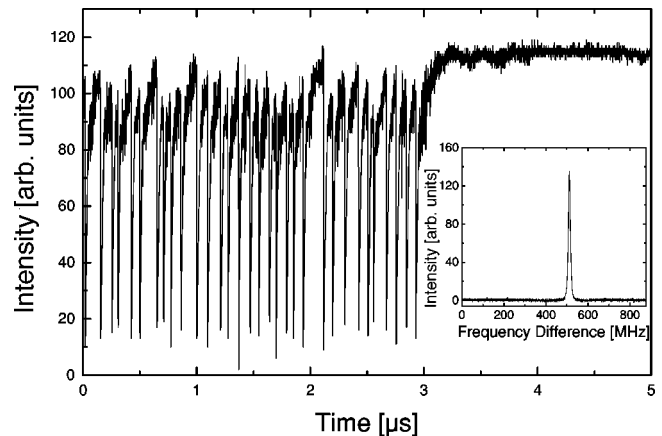


FIG. 4. Intensity time series for  $I = 60 \text{ mA}$  and  $\gamma = 45 \text{ ns}^{-1}$ , showing a transition from LFFs to stable emission on a high-gain external-cavity mode. The inset shows the optical spectrum of the stable emission state recorded by the scanning Fabry-Pérot interferometer.

quent LFF events. Increasing the injection current, the periods of stable emission are prolonged by several orders of magnitude, while the time intervals between the LFF dropouts shorten. On the one hand, this means that in the parameter region right above threshold, the spontaneous emission noise kicks the trajectory off the HGM, as is described in [6]. For higher currents, on the other hand, the duration of the stable states far exceeds the time intervals between two LFF events. The relative strength of the spontaneous emission noise is reduced and, thus, does not, or only very rarely, suffice to push the trajectory away from the stable mode. In case the trajectory is ejected from the HGM by an external perturbation or noise, the system undergoes a varying number of LFF cycles before it returns to one of the HGMs. For high currents within the coexistence region, the duration of the LFF states increase significantly; however, once a HGM is reached, the trajectory remains there for a long time. This behavior indicates that the probability of reaching the HGM in this parameter region is reduced with increasing injection currents. Nevertheless, the trajectory can remain on the HGM, because the level of the spontaneous emission noise is too low to kick the trajectory off the HGM. Outside the coexistence region, finally, the trajectory does not reach the HGM anymore and the system shows nothing but LFF behavior. To sum up, the relative duration of the stable emission state and the LFF state strongly varies with the position of the system in the  $\gamma$ - $I$  space.

We have used an etalon inside the external cavity in order to exclude the influence of multi-diode-mode effects on the dynamical behavior of the system. Comparing the dynamical

behavior with and without the intracavity etalon over the whole accessible parameter space, we find some slight quantitative but no qualitative changes. Shape, size, and position of the various dynamical regions in the  $\gamma$ - $I$  space, including the coexistence regime, remain essentially unchanged. Consequently, we conclude that the number of longitudinal diode modes is not crucial for the mechanism governing the dynamical behavior described in this paper.

In conclusion, we have classified the dynamical behavior of semiconductor lasers subject to optical feedback in a  $\gamma$ - $I$  space diagram providing both detailed information and a global survey about the dynamics of the system. In particular, we have reported, to our knowledge, the first measurement of a large parameter regime in which the LFF phenomenon coexists with stable emission on a single high-gain external-cavity mode. We have provided, thus, experimental evidence for the existence of the HGMs predicted by the theoretical model, based on the Lang-Kobayashi equations, which proposes a deterministic mechanism underlying the LFF. Furthermore, we have shown that the importance of spontaneous emission noise and the probability of reaching the HGM strongly vary over the coexistence region. We conclude that the results presented in this paper confirm the deterministic mechanism underlying the LFF.

Stimulating discussions with M. Münkel, D. Lenstra, C. R. Mirasso, and G. H. M. van Tartwijk are gratefully acknowledged. The authors thank the Deutsche Forschungsgemeinschaft for funding within the SFB 185 "Nichtlineare Dynamik."

- 
- [1] D. Lenstra, B. H. Verbeek, and A. J. den Boef, *IEEE J. Quantum Electron.* **QE-21**, 674 (1985).
  - [2] R. W. Tkach and A. R. Chraplyvy, *J. Lightwave Technol.* **LT-4**, 1665 (1986).
  - [3] M. Pan, B. Shi, and G. R. Gray, *Opt. Lett.* **22**, 166 (1997).
  - [4] J. Mørk, B. Tromborg, and P. L. Christiansen, *IEEE J. Quantum Electron.* **QE-24**, 123 (1988).
  - [5] C. H. Henry, and R. F. Kazarinov, *IEEE J. Quantum Electron.* **QE-22**, 294 (1986).
  - [6] A. Hohl, H. J. C. van der Linden, and R. Roy, *Opt. Lett.* **20**, 2396 (1995).
  - [7] P. Besnard, B. Meziane, and G. Stephan, *IEEE J. Quantum Electron.* **QE-29**, 1271 (1993).
  - [8] F. de Tomasi, E. Cerboneschi, and E. Arimondo, *IEEE J. Quantum Electron.* **QE-30**, 2277 (1994).
  - [9] J. Sacher, W. Elsässer, and E. O. Göbel, *Phys. Rev. Lett.* **63**, 2224 (1989).
  - [10] D. W. Sukow, J. R. Gardner, and D. J. Gauthier, *Phys. Rev. A* **56**, R3370 (1997).
  - [11] T. Sano, *Phys. Rev. A* **50**, 2719 (1994).
  - [12] R. Lang and K. Kobayashi, *IEEE J. Quantum Electron.* **QE-16**, 347 (1980).
  - [13] A. M. Levine, G. H. M. van Tartwijk, D. Lenstra, and T. Erneux, *Phys. Rev. A* **52**, R3436 (1995).
  - [14] C. H. Henry, *IEEE J. Quantum Electron.* **QE-18**, 259 (1982).
  - [15] G. H. M. van Tartwijk, A. M. Levine, and D. Lenstra, *IEEE J. Sel. Top. Quantum Electron.* **1**, 466 (1995).
  - [16] I. Fischer, G. H. M. van Tartwijk, A. M. Levine, W. Elsässer, E. O. Göbel, and D. Lenstra, *Phys. Rev. Lett.* **76**, 220 (1996).
  - [17] J. Mørk, B. Tromborg, J. Mark, and V. Velichansky, *Proc. SPIE* **1837**, 16 (1992).